ARMA 08-123

Void Detection Demonstration: Cross Hole Seismic Tomography

Kieffer, D. S.
Graz University of Technology, Graz, Austria
Hanna, K.
ZapataEngineering, Blackhawk Division, Golden, CO, USA
Bluemel, M.
Graz University of Technology, Graz, Austria

Copyright 2008, ARMA, American Rock Mechanics Association

This paper was prepared for presentation at San Francisco 2008, the 42nd US Rock Mechanics Symposium and 2nd U.S.-Canada Rock Mechanics Symposium, held in San Francisco, June 29-July 2, 2008.

This paper was selected for presentation by an ARMA Technical Program Committee following review of information contained in an abstract submitted earlier by the author(s). Contents of the paper, as presented, have not been reviewed by ARMA and are subject to correction by the author(s). The material, as presented, does not necessarily reflect any position of ARMA, its officers, or members. Electronic reproduction, distribution, or storage of any part of this paper for commercial purposes without the written consent of ARMA is prohibited. Permission to reproduce in print is restricted to an abstract of not more than 300 words; illustrations may not be copied. The abstract must contain conspicuous acknowledgement of where and by whom the paper was presented.

ABSTRACT: Significant hazards to miners are created when active workings approach mined-out areas of either the same mine, or mines located adjacent, above, or below the active mine. Potential hazards include ground collapse and water or toxic gas inundation. These previously mined-out areas may be unintentionally penetrated if information pertaining to their location is not accurate or available to mine operators. To mitigate intersection risks, geophysical techniques offer means to detect the presence of old mine workings before they are encountered. The reliability of cross hole seismic tomography (XHST) was evaluated through a void imaging demonstration at the Colorado School of Mines Edgar Mine experimental facility. Construction of an isolating bulkhead permitted imaging comparisons between air-filled and water-filled void conditions. Despite rather small errors in void location, it is concluded based on imaging results that XHST can offer a reliable and sufficiently accurate method of void imaging for the purpose of mitigating the hazards related to intersecting abandoned mine workings.

1. INTRODUCTION

Significant hazards to miners are created when active workings approach mined-out areas of either the same mine, or mines located adjacent, above, or below the active mine. Potential hazards include ground collapse and water or toxic gas inundation. These previously mined-out areas may be unintentionally penetrated if information pertaining to their location is not accurate or available to mine operators.

Although there are current regulations at the state and federal level addressing the accurate surveying and mapping of mine workings as well as the long-term archival of mine maps, this was not the case prior to approximately 1970. Many of the abandoned mines were in operation prior to the regulations and have not been accurately surveyed, mapped, or documented. In addition, many of the maps that have been created cannot be located.

Mine Safety and Health Administration (MSHA) records show that since 1995, there have been over 100 reported incidents where active mines have inadvertently cut into mined-out areas. Unavailable, inaccurate, or incomplete mapping of older abandoned mines is typically responsible. Many additional incidents have not been officially reported because no injuries or other significant consequences resulted. These incidents continue to occur as mine operators attempt to recover reserves that may be located near abandoned mines.

A mine operator is presently required to identify any adjacent mine that will be within 1,000 feet of the projected workings of the proposed mine. However, investigation of recent inundation incidents has found that maps of abandoned mines have been off by as much as 3,000 feet, meaning that maps alone cannot reliably ensure that inundation will not occur.

Geophysical techniques offer means to detect the presence of old mine workings at a resolution that may be far superior to old mine maps. In this paper, the results of void imaging using cross hole seismic tomography (XHST) are summarized. These surveys were conducted at the Colorado School of Mines (CSM) Edgar Mine experimental facility, located in Idaho Springs, Colorado. Construction of an isolating bulkhead permitted imaging comparisons between air-filled and water-filled void conditions.

2. EDGAR EXPERIMENTAL MINE

The CSM Edgar Mine, was one of the rich gold and silver mines in the Idaho Springs mining district, located approximately 30 miles west of Denver in the town of Idaho Springs (Figure 1)

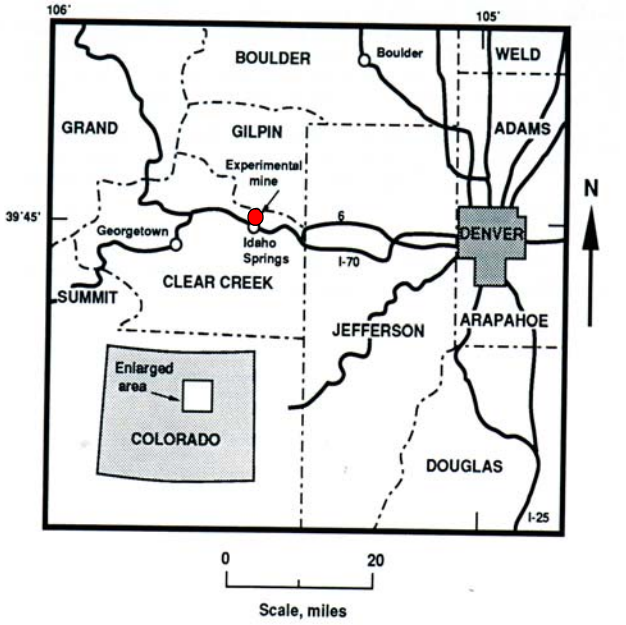

Fig. 1. Edgar Mine location map.

The underground workings of the Edgar Mine comprise a network of horizontal openings having a cumulative length of approximately 1.4 miles. Lengths of individual openings vary from less than 30 feet to approximately 1900 feet, and the cross-sectional dimensions range from about 8-feet wide by 8-feet high, to 15-feet wide by 15-feet high.

2.1 Geologic Overview

The Edgar mine extends through Precambrian rock units which have been subjected to three or more episodes of structural deformation. As shown in Figure 2, principal rock types include quartz-plagioclase gneiss, quartz-plagioclase-biotite gneiss, quartz-biotite-hornblende gneiss and biotite-microcline pegmatites.

The mine is situated on the steeply dipping northwest flank of a northeastward trending anticline and contains many small fault zones. The fault zones generally strike in a northeast direction and dip to the north between 30 and 80 degrees. The rock mass in the area of the mine has at least three joint sets, and in localized areas up to five joint sets. Rocks encountered in the Edgar Mine are generally very competent, being characterized by the geomechanical properties summarized in Table 1.

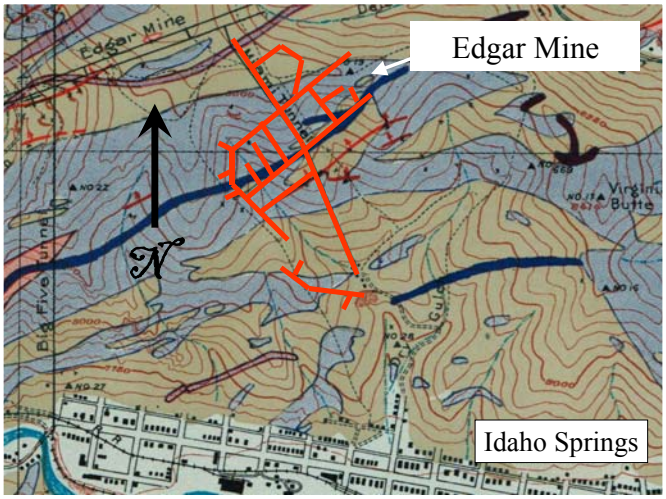

Explanation:
Light Blue: Precambrian quartz-plagioclase gneiss and quartz-plagioclase-biotite gneiss
Brown: Precambrian quartz-biotite-hornblende gneiss and biotite-microcline pegmatites.
Black and Purple: Tertiary porphyry dikes
Dark Blue: Silver veins
Red: Approximate location of the Edgar Mine Workings

Fig. 2: Edgar Mine geology map.

Table 1. Typical geomechanical properties of rock units at the Edgar Mine.

Uniaxial Compressive Strength	40 – 150 MPa
Elastic Modulus	60 to 90 GPa
Poisson's Ratio	0.2
Joint Friction Angle	30º to 45º
Rock Mass Rating (RMR)	40 to 80

3. EXPERIMENTAL SETUP

3.1 Bulkhead Construction

In order to permit void detection under air and water filled void conditions, a reinforced shotcrete bulkhead was constructed. As shown in Figure 3, the bulkhead is located within the Army Tunnel, where it isolates an approximately 100 foot length of drift. All void detection demonstrations were performed using the depicted boreholes U1A and U5, having depths of 275 and 314 feet, respectively.

The drift within the area isolated by the bulkhead (and along a section between Boreholes U1A and U5) has an approximately square cross section, with average edge dimensions of approximately 11 feet as depicted in Figure 4.

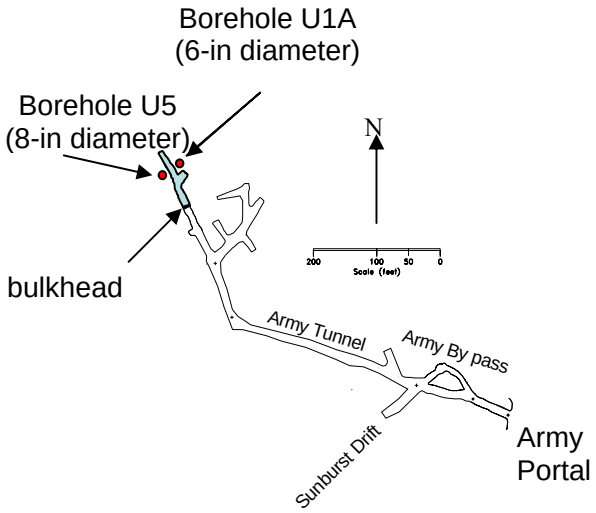

Fig. 3. Location of bulkhead and the boreholes utilized for geophysical investigations.

Fig. 4. Army Tunnel conditions prior to bulkhead construction (future bulkhead location indicated by sidewall anchor bolts).

Photographs of the bulkhead during construction operations are shown in Figure 5. Rock surfaces within the isolated section of the tunnel were left bare, and when filled, the water surface elevation corresponded to the vent pipe inverts noted.

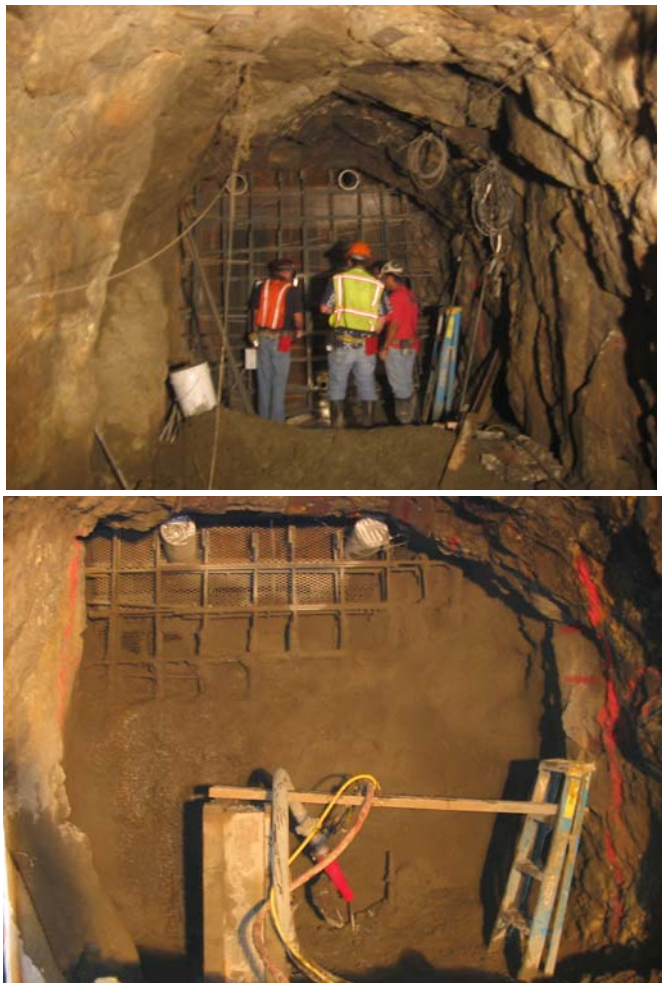

Fig. 5. Bulkhead conditions during construction (note vent pipes at top of bulkhead).

3.2 Borehole Deviation Surveys

To provide necessary spatial constraint, deviation surveys were performed for Boreholes U1A and U5. These boreholes were installed many years ago as part of the U.S. Army's Korean tunnel detection program, and detailed borehole logs were not available for this study. The results of deviation surveys are shown in Figures 6 and 7, and these results were utilized for proper processing of all surveys. Referenced from the top of the boreholes, U1A deviated approximately 3.17 ft to the south and 0.97 ft to the east, and borehole U5 deviated approximately 4.67 ft to the west and 0.59 ft to the north.

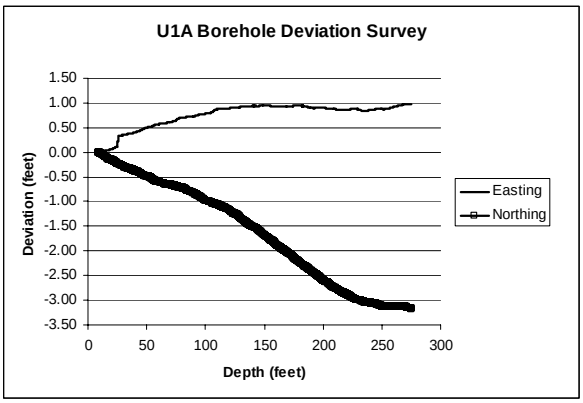

Fig. 6. Borehole deviation survey results for U1A.

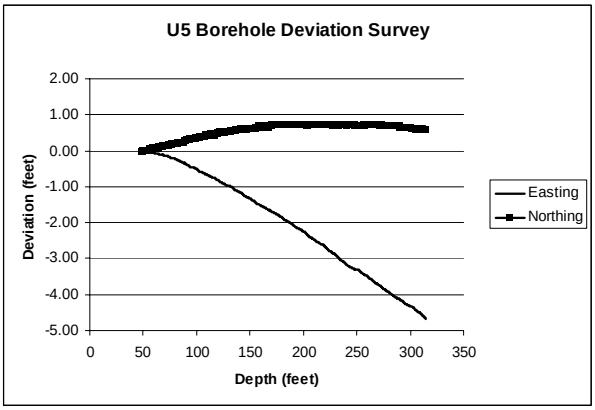

Fig. 7. Borehole deviation survey results for U5.

4. CROSS HOLE SEISMIC TOMOGRAPHY

The objective of this investigation was to conduct two-dimensional cross hole seismic tomography surveys in order to map the location of the tunnel void between Boreholes U1A and U5, and to assess any variation in the dataset corresponding to air and water filled void conditions.

4.1 Theory and Background

Cross hole seismic tomography (XHST) is used for high-resolution imaging of the subsurface between boreholes. Tomography is an inversion procedure that provides for 2-D and 3-D velocity and/or attenuation imaging between boreholes from observation of transmitted first-arrival seismic energy.

Tomography data collection, as shown in Figure 8, involves scanning the region of interest with many combinations of source and receiver depth locations, similar to a medical Computerized Axial Tomography Scan (CATscan). Typical field operation consists of placing a string of receivers (geophones or hydrophones) at the bottom of one borehole and moving the source systematically in the opposite borehole from bottom to top. The receiver string is then moved to the next depth interval and the test procedure is repeated until data from all possible source-receiver combinations are obtained.

The use of tomographic analysis for imaging geological boundaries between boreholes has become a well-established technique in geophysical investigations. It involves imaging the seismic properties from the observation of the transmitted seismic wave (compressional P-wave or shear S-wave), first arrival energy in either time or amplitude. The relationship between the velocity field v (x, y) and travel time t_i is given by the line integral (for a ray i):

$$t_i = I_{Ri}\, ds / v(x,y) \qquad (1)$$

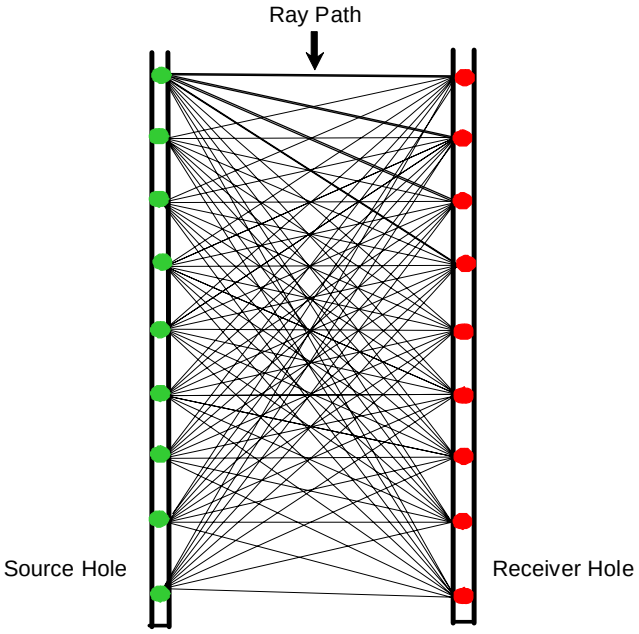

Fig. 8. Basic principle of the XHST technique.

Where R_i denotes the curve connecting a source-receiver pair, which yields the least possible travel time according to Fermat's principle. Tomography is an attempt to match calculated travel times (model responses) to the observed data by inversion of these line integrals. Initially, the region of interest is divided into a rectangular grid of constant velocity cells (j) and a discrete approximation of the line integral is assumed as:

$$t_i = 3_j\, \Delta S_{ij} \,.\, n_j \qquad (2)$$

Where ΔS_{ij} is the distance traveled by ray i in cell j, and n_j slowness within cell j. Using a first order Taylor expansion and neglecting residual error, Eq. (2) can be written in matrix form as:

$$\underline{y} = A\, \underline{x} \qquad (3)$$

Where the vector $\underline{y}$ is defined as the difference between computed travel times (from the model) and the observed travel times, vector $\underline{x}$ is the difference between the true and the modeled slowness, and A is the Jacobian

matrix. In travel time tomography, Eq. (3) is solved using matrix inversion techniques.

The seismic wave field is initially propagated through a presumed theoretical model and a set of travel times is obtained by ray-tracing (forward modeling). The travel time equations are then inverted iteratively in order to reduce the root mean square (RMS) error between the observed and computed travel times. The inversion results can be used for imaging the velocity (travel time tomography) and attenuation (amplitude tomography) distribution between boreholes.

4.2 Data Acquisition

The XHST data were acquired in two separate phases (Phase I & II). Within each phase there were two separate surveys: the first survey was conducted with an air-filled void condition, and the second survey was conducted with a water-filled void condition. There was a delay between each of the surveys in order for water to be pumped behind the shotcrete bulkhead to fill the void.

After a review of the Phase I data and an initial attempt at processing, it was determined that recorded signals were dominated by electronic cross-feed of the signal sent to drive the source, and the data were not of sufficient quality to process as a XHST data set. The Phase I survey was performed with the Etrema swept frequency seismic source (Figure 9)

Fig 9. Etrema swept frequency seismic source.

Phase II, a repeated survey utilized a sparker source (Figure 10), and the data quality for this survey was much higher and suitable for processing as an XHST data set.

Fig. 10. Sparker seismic source.

The cross hole tomography survey was conducted between boreholes U1A and U5, having a horizontal offset of approximately 35 ft at the ground surface. The top of the target void for the survey is located at an elevation of 7879 ft, or at an approximate depth of 200 ft below ground surface. The average dimension of the void is approximately 11-ft by 11-ft in the 2-D plane formed by connecting the survey boreholes. This site is well suited for the evaluation of the XHST method because the depth and dimension of the void is well known. Survey data was collected with the equipment and acquisition parameters summarized in Table 2

Table 2. XHST data acquisition and equipment parameters.

Acquisition System	Geometrics Stratavisor NX 60 channel - 0.25 ms sampling and 64 ms record length
Seismic Source	1st Attempt: Etrema Swept Frequency Source with Agilent Signal Generator and 250 watt amplifier sweeping 40 to 500 Hz.
	2nd Attempt: Down hole Sparker using Applied Acoustics CSP1500 Signal Generator – 3 source stacks per station at 800 joules output per shot
Source Interval	3 feet
Hydrophones	Oyo Geospace 12 channel @ 3-ft spacing and/or Benthos 24 channel string @ 1-m spacing

As discussed above, an initial attempt was made to acquire the dataset using the Etrema swept frequency source. However, the data quality was insufficient to accurately pick the travel time (first breaks). The reasons for this were as follows:

(i) There was a significant amount of crosstalk from the Etrema source amplifier that appears to be significantly higher in amplitude than any seismic signal received by the hydrophones. This problem was not detected during data acquisition because correlation was not possible in the field.

(ii) Due to the close spacing of the boreholes and the high seismic velocities of the rock strata surrounding the void, the first arrival time is very close to the beginning of the records (less than 5 ms), when using a vibratory source such as the Etrema, the correlated wavelet can be truncated by the beginning of the record.

The data were obtained by lowering the hydrophone string in borehole U5 and then acquiring seismic records with the source located at different depths in borehole U1A. To facilitate source and receiver performance, water was added to the initially dry boreholes. As shown schematically in Figure 11, data were acquired over depths in the boreholes corresponding to about 51 feet above to 63 feet below the target void (approximate survey elevations 7930 to 7805 feet).

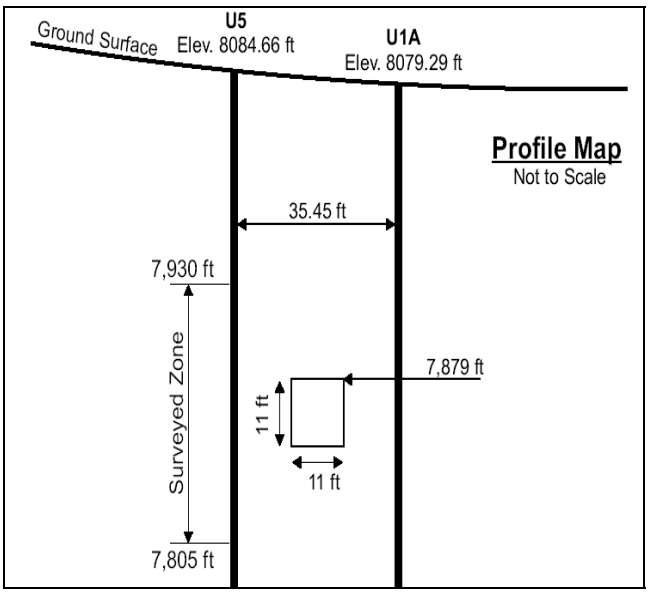

Fig. 11. Schematic vertical profile of boreholes U1A and U5, the target void, and surveyed zone.

Figure 12 shows the 24-channel hydrophone array being lowered in borehole U5, and Figure 13 shows the data acquisition setup and water being added to borehole U1A.

Fig. 12. The 24-channel hydrophone array.

Fig. 13. Data acquisition setup, with water being added to borehole U1A.

4.2 Data Processing and Interpretation

The survey data, corrected for borehole deviations, were imported into Oyo Seisimager, where the source and receiver geometry were applied and the first arrival times picked. The first arrival time files were then exported, reformatted and input into GeotomCG, where the final tomograms were generated. GeotomCG uses the simultaneous iterative reconstruction technique (SIRT) algorithm [1].

GeoTomCG allows for 3-D processing and can account for positional variation based on borehole deviation data. The basic data processing flow included the following:

- Import data;
- Frequency filter to remove noise;
- Pick first breaks;
- Apply geometry and import into tomographic software package;
- Edit data for outliers;
- Create starting model (average constant velocity);
- Set inversion parameters (curving ray, velocity limits, number of iterations);
- Invert data while observing changes in RMS error and residuals;

- Determine appropriate number of iterations;
- Export final model;
- Edit final model format and import into Geosoft Oasis;
- Grid and display model; and
- Export final image.

The final inversion parameters that appeared to give the best results were:

- 5 Straight ray inversion steps, followed by up to 10 curved ray;
- Velocity constraints of no less than 5,000 ft/sec and no more than 18,000 ft/sec;
- Pixel size of 1 m was used based on the spacing of the shots and receivers;
- Final RMS (root mean square) residuals for the GeotomCG inversions were on the order of $3.5x10^{-4}$.

The sparker source provided good signal amplitude and high frequency response. Figure 14 shows an example shot record recorded during the field survey. The source was positioned at a depth of 197 ft and the hydrophone receivers were positioned between 182 ft and 215 ft depth. The trace spectra of this shot record are shown in Figure 15. The spectra show that the sparker produced recorded signals with frequencies ranging from about 400 Hz to 1,500 Hz. The dominant frequency of the first arrival of energy in the shot record is approximately 1,000 Hz.

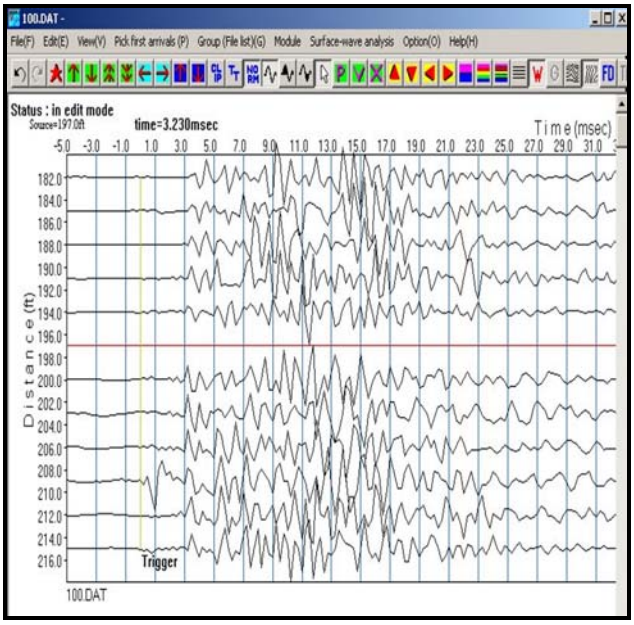

Fig. 14: Sample shot records using the sparker source and hydrophone string.

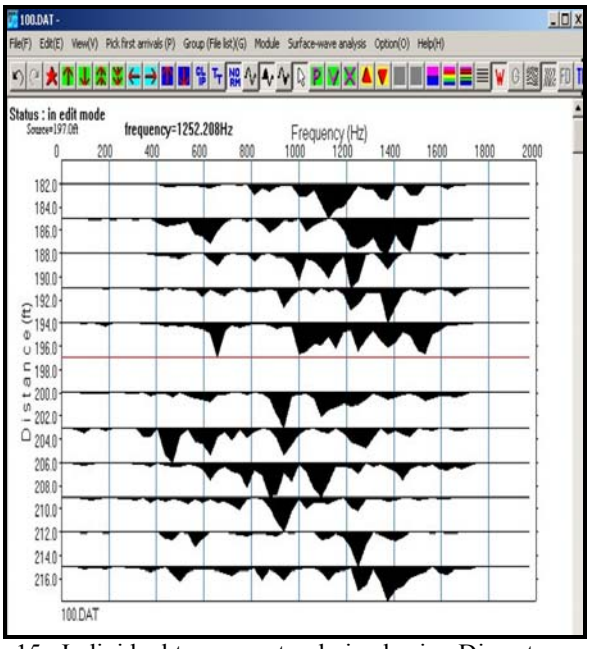

Fig. 15: Individual trace spectra derived using Discrete Fourier Transform.

Source time repeatability was visually monitored during data acquisition, but specific repeatability test records were not recorded. During the survey, three shots were stacked (vertically summed) for each shot record. Good repeatability of source timing can be inferred by the high frequency signals found in the spectra of the shot records. Stacking shots using a source with poor repeatability in shot timing produces summed records with coherent signals (i.e. first arrivals) that have lower effective frequency content than found in a single shot record. The high frequency of the stacked data suggests good source timing repeatability.

Figure 16 and 17 show the 2-D velocity tomograms between boreholes U1A and U5 for the air- and water-filled void conditions, respectively. Lower velocity zones in the tomograms are shown as "cooler" colors (blue and green), and higher velocity zones in the tomograms are shown as "warmer" colors (red and pink). The low velocity anomaly interpreted as the void in Figure 16 for the air-filled void is approximately located in the center of the tomogram with the top of the anomaly at an elevation of about 7887 feet. The low velocity anomaly interpreted as the void in Figure 17 for the water-filled void is approximately located in the center of the tomogram with the top of the anomaly at an elevation of approximately 7882 feet. As a comparison, the true top of void elevation is at an approximate elevation of 7879 feet.

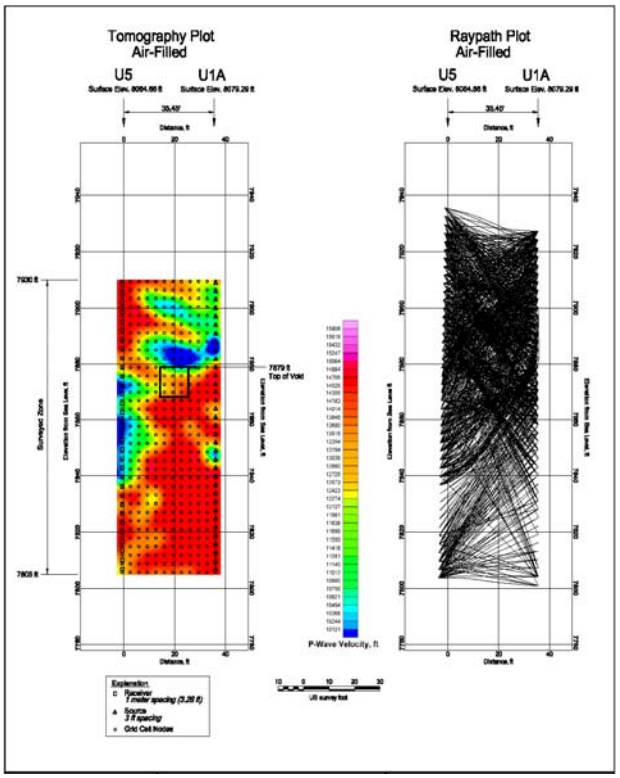

Fig. 16. Two-dimensional tomogram image for the air filled void condition.

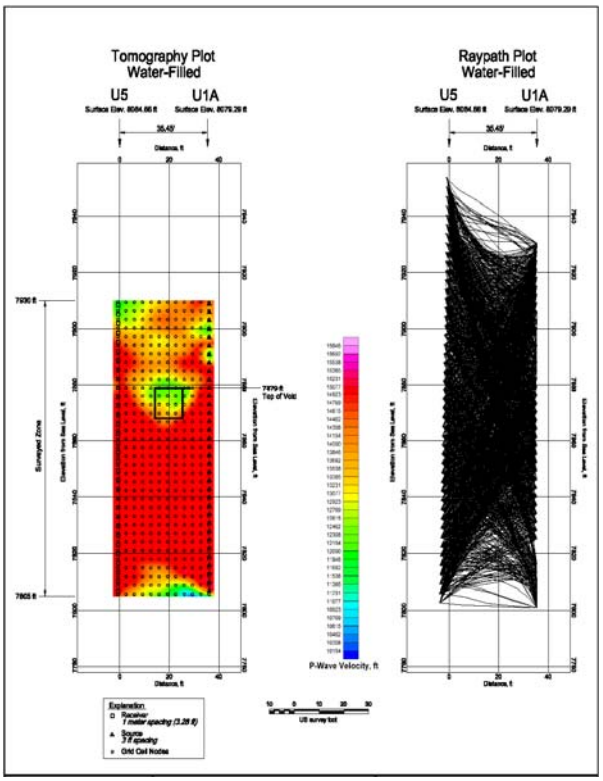

Fig. 17. Two-dimensional tomogram image for the water filled void condition.

5. DISCUSSION AND CONCLUSIONS

The low velocity anomalies interpreted as the target void are located above the known void elevation, with vertical offsets ranging from about 3 to 8 feet. These differences, in part, may be due to the irregular shape of the void, fractures/loosening around the void due to tunnel driving, or due to the effects of the tomographic inversion algorithm and gridding. However, it appears from both the raw seismic records and the final tomograms that the data quality acquired with the water-filled void was better than that of the air-filled void. This is likely due to less attenuation of the signal prorogating through the rock strata surrounding the water-filled void than the air-filled void condition. Therefore, the travel time measurements were more accurate, allowing a better inversion. Saturated fractures between the boreholes due to water leakage from the void may have reduced signal attenuation, providing for higher signal-to-noise ratio data and higher frequency content. This may also be attributed to decreased signal scattering from the void/rock interface due to the lower acoustic impedance between water/rock versus air/rock boundary.

The results of the survey indicate that the presence of the void could be detected using XHST under both air filled and water filled conditions. In both cases, a low velocity zone was present between the boreholes that correlated reasonably well with the location of the known void. Other low velocity zones were present above the void, which may indicate the presence of fracturing/loosening within the rock mass. When the boreholes were filled with water, there was significant leakage from the boreholes indicating that open fractures are present in this area.

Other conclusions drawn from the investigation include:

- Reacquiring the data using a sparker versus the swept frequency Etrema source provided significantly better data quality. It appears that there was significant cross-talk between the source input signal and the receivers, that was not evident in the uncorrelated field records during the Etrema data acquisition.

- The use of the new 24-channel hydrophone string provided improved signal-to-noise content than the 12-channel string used in the Phase I data collection.

In general, the XHST technology was successful in detecting the location of the void at this site. Had detailed borehole logs been available, inhomogeneities in the rock mass may have become apparent, and modeling of such inhomogeneities may have resulted in improved accuracy of the results. Despite rather small errors in void location, it is concluded based on imaging results that XHST can offer a reliable and sufficiently

accurate method of void imaging for the purpose of mitigating hazards related to intersecting abandoned mine workings.

6. ACKNOWLEDGEMENTS

Financial support for the work described herein was provided by the U.S. Department of Labor, Mine Safety and Health Administration under contract award No. B2532537.

REFERENCES

1. Lytle, R.J., K.A. Dines, E.E. Laine, and D.L. Lager, 1978, Electromagnetic Cross-Borehole Survey of a Site Proposed for an Urban Transit Station. UCRL-52484, Lawrence Livermore Laboratory, University of California, 19 pp.